Construction and Building Materials 252 (2020) 119055

Contents lists available at ScienceDirect

Construction and Building Materials

journal homepage: www.elsevier.com/locate/conbuildmat

Effect of temperature on geopolymer and Portland cement composites modified with Micro-encapsulated Phase Change materials

Shima Pilehvar [a], Susana G. Sanfelix [a,b], Anna M. Szczotok [a], Juan Francisco Rodríguez [c], Luca Valentini [d], Marcos Lanzón [e], Ramón Pamies [f], Anna-Lena Kjøniksen [a,*]

[a] Faculty of Engineering, Østfold University College, P.O. Box 700, 1757 Halden, Norway
[b] Departamento de Química Inorgánica, Universidad de Málaga, Campus Teatinos s/n., 29071 Málaga, Spain
[c] Department of Chemical Engineering, University of Castilla – La Mancha, 13004 Ciudad Real, Spain
[d] Department of Geosciences, University of Padua, 35131 Padua, Italy
[e] Departamento de Arquitectura y Tecnología de la Edificación, Escuela Técnica Superior de Arquitectura y Edificación ETSAE, Universidad Politécnica de Cartagena, 30203 Alfonso XIII 52, Cartagena, Spain
[f] Departamento de Ingeniería Mecánica, Materiales y Fabricación Universidad Politécnica de Cartagena, Cartagena, Murcia, Spain

HIGHLIGHTS

- Microcapsules slow down the reaction of both geopolymer and Portland cement pastes.
- Increasing the temperature accelerates the setting times of geopolymer and Portland cement pastes.
- Addition of microcapsules reduces the compressive strength.
- Enhanced porosity at higher temperatures for both geopolymer and Portland cement.

ARTICLE INFO

Article history:
Received 13 August 2019
Received in revised form 30 March 2020
Accepted 5 April 2020
Available online 11 April 2020

Keywords:
Micro-encapsulated Phase Change Materials
Portland cement
Geopolymer
Microstructure
Compressive strength
Isothermal calorimetry

ABSTRACT

To reduce pollution and global warming, the energy consumption needs to be decreased. Incorporation of Phase Change Materials (PCMs) into building materials can help lower the energy needed to cool and warm buildings, while keeping the indoor temperature at a comfortable level. However, incorporation of PCMs into construction materials alter their performance. In this study, the effect of temperature and addition of two different Micro-encapsulated Phase Change Materials (MPCM) to geopolymer concrete (GPC) and Portland cement concrete (PCC) and pastes was investigated. The samples were examined both below (20 °C) and above (40 °C) the melting points of the PCMs. While the MPCM is not damaged by the alkaline solution, a few microcapsules are broken during the mixing process. Isothermal calorimetry shows that MPCM addition slows down the reaction rate of both geopolymer and Portland cement paste. The setting times were faster when the temperature was increased. The mechanical properties are reduced when MPCM is added to GPC and PCC, although the compressive strength is adequate for building applications. Microstructural studies show more uniform and undamaged edges in the shell-concrete matrix transition zone of GPC than PCC. The samples cured at 40 °C exhibits more air voids in both GPC and PCC than at 20 °C.

1. Introduction

The production of Portland cement is a major contributor to CO_2 emissions [1]. One of the efforts to reduce the CO_2 produced by concrete is to develop geopolymer-based building materials, consisting of inorganic alumino-silicate polymers [2]. Geopolymerization is an exothermic reaction that involves dissolution of silico-aluminates in an alkaline solution and provides an amorphous to semi-crystalline three-dimensional network [3]. The aluminosilicate sources can be natural minerals, like kaolinite, metakaolin and clays [2,4] or industrial secondary products such as fly ash (FA), ground granulated blast furnace slag (GGBFS), red mud, and silica fume [5–7]. Sodium hydroxide (NaOH), sodium silicate (Na_2SiO_3), potassium hydroxide (KOH), and potassium silicate (K_2SiO_3) are commonly used as the alkaline solutions. Generally, geopolymer concrete (GPC) exhibits improved mechanical

* Corresponding author.
E-mail address: anna.l.kjoniksen@hiof.no (A.-L. Kjøniksen).

https://doi.org/10.1016/j.conbuildmat.2020.119055
0950-0618/

performance in comparison with conventional Portland cement concrete (PCC) [8,9].

Buildings accounts for approximately 1/3 of the global energy demand and about 30% of CO_2 emissions, and more than 50% of the energy use of buildings is heating and cooling [10]. Accordingly, obtaining new building materials containing Phase Change Materials (PCMs) is attracting interest, to reduce the energy consumption while retaining comfortable indoor temperatures [11–13]. PCMs are compounds that absorb, store and release energy during the phase change within a specific temperature range. When the temperature of the environment rises above the melting point of the PCMs, the PCMs absorb heat while changing from solid to liquid. When the temperature decreases below the melting point of the PCMs, the heat of fusion is released back to the environment and the PCMs return to a solid state [14]. In hot climates such as southern Europe, PCMs prevent buildings from overheating at daytime during the warm season, and may also attenuate the necessity for heating at night during the cold months [15–18]. PCMs with melting points in the range of 10 to 30 °C should be used to facilitate human thermal comfort[19]. Microencapsulation of PCMs is conducted to avoid interactions between the PCMs and the surrounding environment, to provide a high heat transfer area, and to prevent leakage of the core material during the phase change [20].

In order to obtain new structural materials with improved thermal energy storage, Micro-encapsulated Phase Change Materials (MPCM) have been incorporated in concrete [21,22]. However, the mechanical properties of concrete are diminished with the addition of MPCM [23–26]. Despite reduced concrete compressive strength after adding MPCM, the compressive strengths are mainly within the desired range (25 to 40 MPa) suitable for constructional purposes [27].

Studies of the mechanical strength of geopolymer [26,28,29] and Portland cement [21,26,30] composites with incorporated MPCM have been reported previously. In addition, their ability to enhance the thermal properties of the building materials for reducing the energy needed to keep a comfortable indoor temperature has been explored [31–35]. However, there are few previous studies utilizing isothermal calorimetry to examine the influence of the addition of MPCM on the reaction kinetics of Portland cement [36,37], and such studies of geopolymers seems to be lacking.

The aim of this study, is to evaluate how incorporation of different types of MPCMs, above and below the melting point of each PCM influences the reaction rates, physical and mechanical properties and the microstructure of both geopolymer and Portland cement composites. This is a continuation of our previous studies [26,38,39], where the effect of MPCMs on the slump, setting times, microstructure, mechanical strength, and the effect of freeze–thaw cycles had been studied. We have also previously examined rheological properties of pre-set Portland cement and geopolymer pastes containing MPCM [40,41], and the thermal properties of PCC and GPC containing MPCM [31–35]. Unlike the previous studies, this paper focuses on how MPCM addition affect the reaction kinetics of the samples, utilizing isothermal calorimetry at both 20 and 40 °C. In order to gain additional information, setting times and compressive strengths are examined at the same temperatures, and finally scanning electron microscopy (SEM) and X-ray tomography were utilized to explore how the microstructure of the samples were affected by MPCM addition at these conditions. Two different MPCMs were compared: PE-EVA-PCM has an amphiphilic polymer shell of low-density polyethylene (50 wt%) and ethylvinylacetate (50 wt%), while St-DVB-PCM has a hydrophobic polymer shell of styrene (50 wt%) and divinylbenzene (50 wt%). Both MPCMs have a paraffin core, with slightly different melting points.

2. Materials and methods

2.1. Materials

In order to prepare geopolymer composites, an alkaline activator solution, class F fly ash (FA), ground granulated blast furnace slag (GGBFS), sand, and gravel were used. The alkaline solution consisted of sodium hydroxide pellets and sodium silicate solution (35 wt% solid). A poly-naphthalene sulfonate polymer (FLUBE OS 39) was used as a superplasticizing admixture to improve the workability of GPC and decrease the amount of water. Portland cement II mixed with FA, was used for Portland cement composites preparation. Dynamon SR-N, which is a high-performance superplasticizing admixture based on modified acrylic polymers, was utilized to improve the workability of PCC. The densities and suppliers of the utilized materials are shown in Table 1. The composition of the fly ash class F (FA) is 50.83 wt% SiO_2, 23.15 wt% Al_2O_3, and 6.873 wt% CaO. The ground granulated blast furnace slag (GGBFS) consists of 34.51 wt% SiO_2, 10.3 wt% Al_2O_3, and 42.84 wt % CaO. Portland cement II (Blaine fineness of 4500 cm^2/g) was pre-mixed mixed with FA from the supplier.

In this study, two different MPCMs denoted PE-EVA-PCM and St-DVB-PCM were utilized. The synthesis of these microcapsules is described in previous publications [42,43]. The properties of the MPCMs are summarized in Table 2. St-DVB-PCM has a hydrophobic shell, while the shell of PE-EVA-PCM is amphiphilic (both hydrophilic and hydrophobic groups). The workability of the pre-set samples becomes poorer with the addition of MPCM [38]. Enhanced hydrophobicity of the MPCM shell reduces the amount of water adsorbed onto the microcapsules [38,40], so that less water is needed to obtain a good workability [38,40,41]. PCMs with melting points around 28 °C and 24 °C were chosen, since this is within the range considered optimal in cooling dominant climates [44].

In order to distinguish the differences in shape and size of the components, SEM images of fly ash, slag, cement, and the two different kinds of microcapsules are provided in Fig. 1. While PE-EVA-PCM reveals a cluster structure due to a high amount of agglomerates, a spherical shape is observed for St-DVB-PCM [26,34]. The PE-EVA-PCM clusters are mainly due to non-encapsulated PCMs [45].

2.2. Specimen preparation

An alkaline solution consisting of a mixture of a sodium silicate solution (35 wt% solids, from VWR, Norway) and 14 M NaOH(aq) (prepared from sodium hydroxide pellets, from VWR, Norway) at a ratio of 1.5 was used for all geopolymer samples [38]. The

Table 1
Densities and suppliers of the utilized materials.

Component	Density (g/cm^3)	Supplier
Class F fly ash	2.26	Norcem, Germany
Ground granulated blast furnace slag	2.85	Cemex, Germany
Portland cement II mixed with FA	3.00	Norcem, Norway
Sand	2. 70	Gunnar Holth AS, Norway
Gravel	2.62	Skolt Pukkverk AS, Norway
Sodium hydroxide pellets	2.13	VWR, Norway
Sodium silicate solution (35 wt% solid)	1.93	VWR, Norway
FLUBE OS 39	1.20	Bozzetto Group, Italy
Dynamon SR-N	1.10	MAPEI, Norway

Table 2
Properties of the two MPCMs [42,43].

Properties	PE-EVA-PCM	St-DVB-PCM
Shell composition	Low density polyethylene (50 wt%) ethylvinylacetate (50 wt%)	Styrene (50 wt%) Divinylbenzene (50 wt%)
Core material	Paraffin	Paraffin
Water affinity	Amphiphilic	Hydrophobic
Melting point	28.4 ± 0.9 °C	24.2 ± 0.9 °C
Latent heat	98.1 J/g [42]	96.1 J/g [43].

alkaline solution was prepared 1 day in advance to ensure complete dissolution of NaOH pellets and to lose the exothermic reaction heat. The microcapsules were added to the paste and concrete by the MPCM additive method and the MPCM replacement method, respectively [26]. The MPCM is added as an extra additive (in volume) to the powder materials in the additive method [46]. In the replacement method, a certain percentage of sand (in volume) is replaced with the same percentage of MPCM [46]. The replacement method cannot be used for the pastes, since they do not contain any sand.

2.2.1. Paste preparation

For geopolymer paste, the alkaline solution and geopolymer binder (Fly ash + slag) was utilized at a ratio of 0.4. For Portland cement paste, a fixed water to cement ratio of 0.35 was used. In the case of the isothermal conduction calorimetry, the materials containing the MPCM were weighed in the calorimeter glass ampoules and loaded into the isothermal conduction calorimeter channels without mixing. In the setting times measurements, the geopolymer binder and alkaline solution (for geopolymer paste) and cement and water (for Portland cement paste) were mixed for 90 s. After the subsequent addition of the microcapsules, the samples were mixed for another 90 s, resulting in homogenous pastes with the same consistencies.

2.2.2. Concrete preparation

The ratio between the liquid (alkaline solution + extra water) and the geopolymer binder, as well as the water to cement ratio of Portland cement were both kept at the same value of 0.5. Additionally, the total amount of sand and gravel for the concrete samples not containing MPCM was approximately the same for GPC and PCC. More details regarding the sample preparation can be found in Pilehvar et al. [26,38]. The amount of MPCM in the samples were chosen based on previous studies [26,34,35,38], with the aim of maximizing the thermal storage capacity while keeping the workability of the pre-set samples and the mechanical strength of the concrete within an acceptable range. The components of the Portland cement and geopolymer mixtures are shown in Table 3 and Table 4, respectively.

2.2.3. Casting and curing

GPC and PCC where 0 and 20% of the sand was replaced by MPCM, were cast into 10 × 10 × 10 cm^3 molds; see Pilehvar et al. [26] for details. After a 24 h precuring period at room temperature with a 90% relative humidity, both GPC and PCC samples were demolded and cured in water at 20 or 40 °C (below and above the melting point of both MPCMs) for 1, 7, 14, and 28 days.

2.3. Testing methods

2.3.1. MPCM shell resistance against alkaline solution and mixing process

To determine the resistance of the MPCM shell against the strong basic environment of the alkaline solution, St-DVB-PCM was immersed in alkaline solution for 7 days. EDX mapping and SEM images of St-DVB-PCM after immersion were performed by scanning electron microscopy (SEM), Hitachi S3500N microscope. Additionally, SEM images of St-DVB-PCM after mixing with aggregates and water for 3 min were utilized to explore whether the mixing process affects the shell of the microcapsules. This experiment was only conducted on St-DVB-PCM, since the irregular

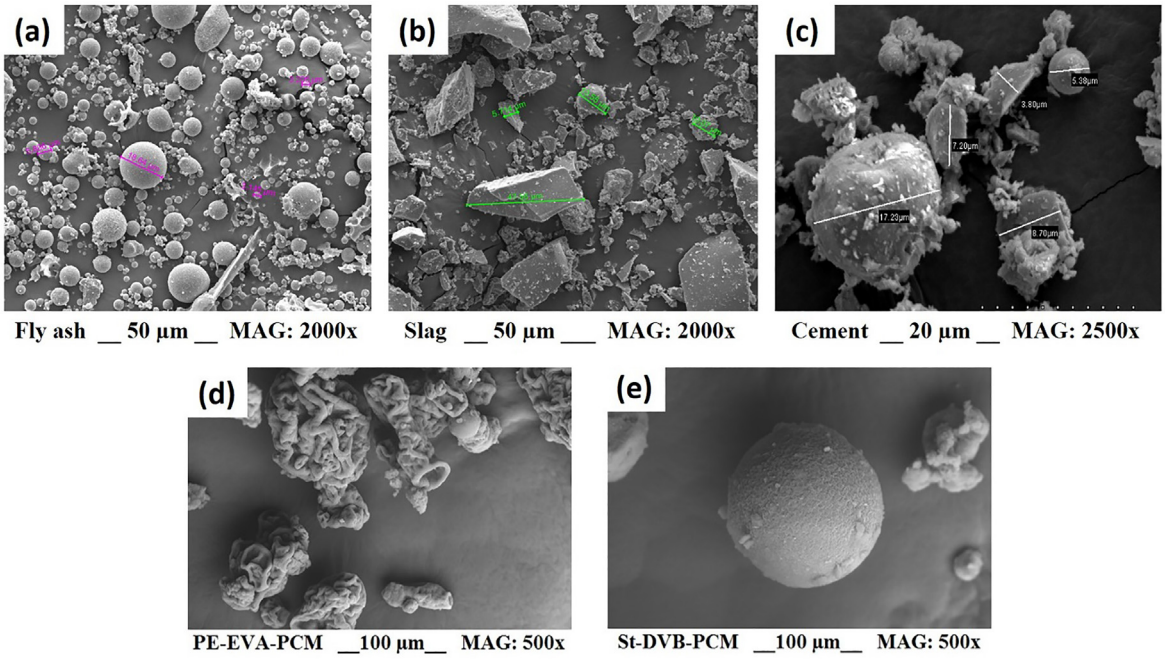

Fig. 1. SEM images of (a) fly ash, (b) Slag, (c) Portland cement, (d) PE-EVA-PCM, and (e) St-DVB-PCM.

Table 3
Composition of the geopolymer composites.

Materials	Paste (kg)		Concrete (kg)	
	MPCM 0%	MPCM 20%	MPCM 0%	MPCM 20%
Alkaline solution	188.5	188.5	189.8	189.8
Fly ash	280.2	280.2	280.2	280.2
GGBFS	191	191	191	191
Sand	–	–	828.1	662.5
Gravel	–	–	809.6	809.6
Extra water	–	–	47	47
Superplasticiser	–	–	4.8	4.8
MPCMs	0	35	0	55.8

Table 4
Composition of the Portland cement composites.

Materials	Paste (kg)		Concrete (kg)	
	MPCM 0%	MPCM 20%	MPCM 0%	MPCM 20%
Cement	471.2	471.2	471.2	471.2
Water	212	212	235.6	235.6
Sand	–	–	957	765.6
Gravel	–	–	705	705
Superplasticiser	–	–	4.8	4.8
MPCMs	0	28.3	0	64.3

shape of PE-EVA-PCM (Fig. 1d) makes it difficult to distinguish whether the shell is damaged during the mixing process.

2.3.2. Isothermal conduction calorimetry

The effect of different MPCMs on the heat evolution of the geopolymer and hydration reactions was studied in an eight-channel isothermal conduction calorimeter (TAM Air instrument) using Admix glass ampoules. All materials were mixed inside the calorimeter channels, after equilibrating them within the calorimeter at the measuring temperature for 24 h. The calorimetry was conducted on geopolymer and Portland cement pastes containing 0% and 20% MPCM. The heat flow was collected for 3 days from the start of the reaction at both 20 °C and 40 °C. As mentioned in in section 2.2, the MPCM is added as an extra additive (in volume) to the fixed binder mass (additive method).

2.3.3. Setting time

A computer controlled Vicat needle apparatus (ToniSET One, Model 7301) was utilized to measure the initial and final setting times in accordance with EN 196–3. The measurements were performed on geopolymer and Portland cement pastes without microcapsules and containing 20% MPCM at both 20 °C and 40 °C. In order to measure the setting times at 40 °C, the basin was filled with water and the conical mold containing the paste was kept inside this basin, which was kept at 40 °C by water circulation through a thermal bath allowing temperature control (±0.1 °C). The setting times was measured at intervals of 2 min and 10 min for geopolymer paste and Portland cement paste, respectively. The initial setting time was defined as when the needle penetration is less than 39.5 mm, and the final setting time at a penetration of 0.5 mm.

2.3.4. Compressive strength

The compressive strength was measured at 40 °C by thermally insulating the compressive strength machine and connecting it to a heating chamber. The compressive strength tests were performed in accordance with EN 12390–3. To remove excess water before initiating the measurements, the cubes cured at 40 °C were kept in a heating chamber at 40 °C for 1 h before being weighed and tested. Three cubes were used for each sample to obtain the reported averages. For comparison purposes, measurements were also carried out at 20 °C.

2.3.5. Microstructural studies

Scanning electron microscopy (SEM) (Hitachi S3500N) was used in order to analyze the morphology of the fracture surface of GPC and PCC specimens without MPCM and with 20% St-DVB-PCM or PE-EVA-PCM cured at 40 °C. The SEM images were captured at 15 kV using back scattered electrons (BSE) to improve the examination of chemical differences on the samples surface.

The internal visualization of the specimens was performed by X-ray tomographic scans. The measurements were conducted by a Bruker Skyscan 1172 CT scanner utilizing 85 kV incident radiation, a rotation step of 0.3°, and 800 ms exposure time per frame. The measurements were performed on cylindrical samples (1 cm height and 1 cm diameter) of PCC and GPC without microcapsules and with 20% MPCM cured at 40 °C.

3. Results and discussion

3.1. MPCM shell resistance against alkaline solution and mixing process

EDX mapping and SEM images of St-DVB-PCM after immersion in the alkaline solution are presented at two different magnifications in Fig. 2a and b. As previously observed for other types of microcapsules [47], the MPCM are resistant to the alkaline solution since no broken or damaged particles are observed in Fig. 2. In addition, the capsules surface is mostly displayed in blue (color assigned to C in Mapping) suggesting that the shell does not retain significant amounts of alkaline solution due to the hydrophobic nature of the shell. Additionally, MPCMs are clearly surrounded by a Na-rich phase. High NaOH concentration in the alkaline solution might cause Na_2CO_3 formation (by carbonation due to atmospheric CO_2).

SEM images of St-DVB-PCM after mixing with aggregates and water for 3 min is shown in Fig. 3, to scrutinize whether the mixing process affect the shell of the microcapsules. It is evident that the mixing process can cause ruptures on the microcapsule shell. A broken MPCM and possible surface damage can be seen in Fig. 3a

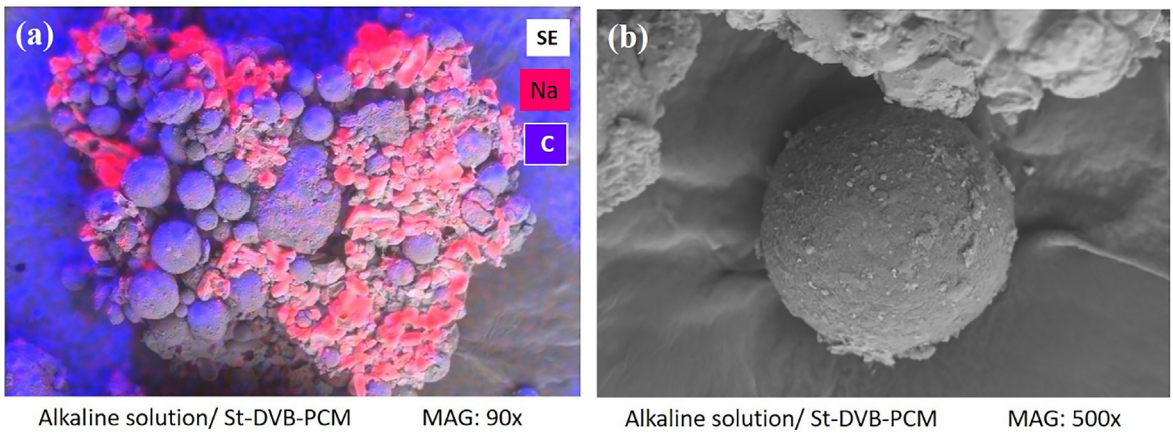

Fig. 2. (a) EDX a cluster of St-DVB-PCM immersed in alkaline solution (b) SEM image of a single particle of St-DVB-PCM after immersing in alkaline solution for 7 days.

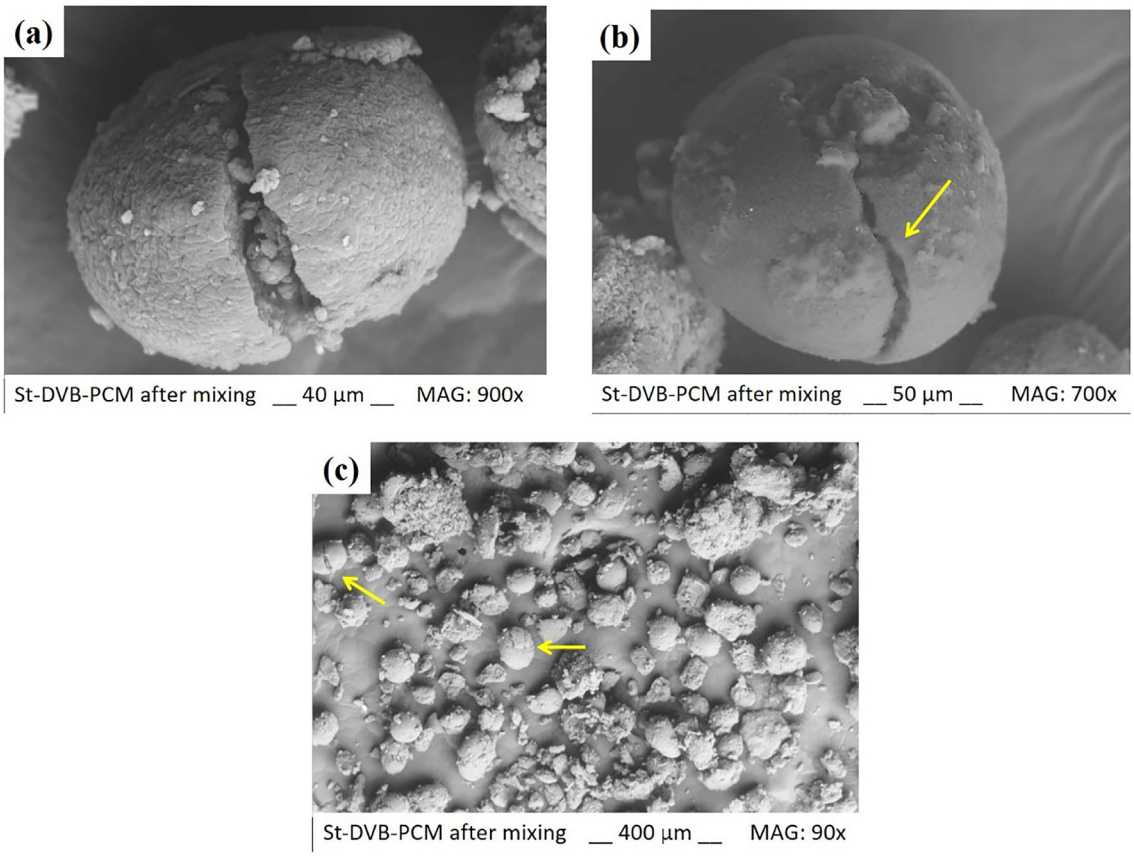

Fig. 3. SEM images of the St-DVB-PCM after mixing (a) at a magnification of 900x, (b) at a magnification of 500x (the arrow shows partial surface damage of the shell), and (c) at a magnification of 90x (the arrows show that some microcapsules are broken).

and b, respectively. However, from Fig. 3c, with a wider field of view, it is clear that only a few microcapsules are broken or damaged during the mixing process. The MPCMs have less stiffness and strength than the aggregates. This might cause deformation and fracture of the MPCM during mixing, which will contribute to lowering the compressive strength of concrete [26]. It should be noted that the field of view is limited, and it is therefore difficult to estimate the percentage of broken MPCM. The irregular shape of PE-EVA-PCM makes it difficult to distinguish between damaged and undamaged shells. These experiments were therefore conducted only on St-DVB-PCM microcapsules.

3.2. Isothermal conduction calorimetry

The rate of reactions in geopolymer and Portland cement pastes without MPCM and with 20% of St-DVB-PCM and PE-EVA-PCM was studied by isothermal conduction calorimetry. In order to evaluate if the reactions are affected by whether the PCMs are in a solid or liquid state, experiments were conducted at 20 °C and 40 °C for 72 h. For geopolymer paste, the first peak in Fig. 4a has been reported to be related to wetting and dissolution of FA and GGBFS [48–51]. Comparison with rheological data on similar geopolymer pastes suggest that geopolymer precursors (monomers) are also

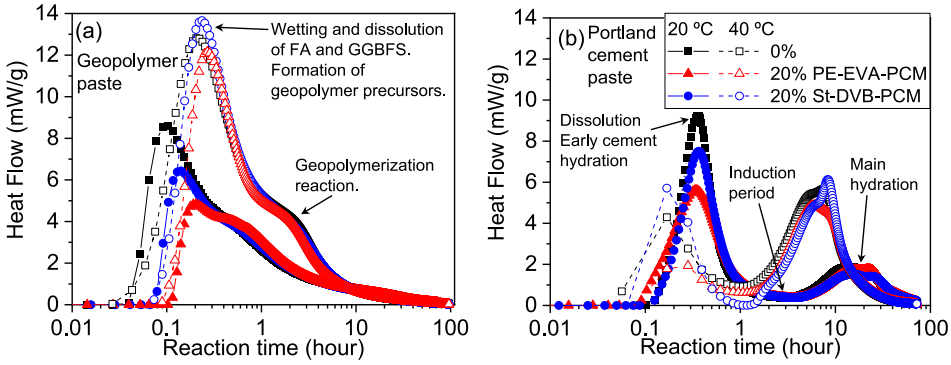

Fig. 4. Heat flow versus reaction time for (a) geopolymer paste and (b) Portland cement paste.

formed at this stage [40]. The shoulder observed at longer times is a second peak, which overlaps with the first peak. This second peak is due to the geopolymerization reaction [40,51]. As can be seen from Fig. 4a, geopolymer dissolution and formation of geopolymer precursors starts within the first 10 min after mixing materials at both 20 °C and 40 °C. However, the heat evolution peak at 40 °C was higher in this step since more FA and GGBFS can dissolve at high temperatures. Interestingly, both the first and second peak are shifted towards longer times when the temperature of the geopolymer paste is raised, even though higher temperatures is expected to speed up reaction rates. This is probably because the dissolution step and the formation of geopolymer precursors can continue for a longer time at high temperatures (shifting the top of the first peak to longer times). The formation of more geopolymer precursors enhances the viscosity of the samples. Accordingly, the transportation of the monomers is slowed down, and the 3D geopolymer network takes longer to form [40] (shifting the second peak to longer times).

For Portland cement (Fig. 4b), there is a first peak related to dissolution and early cement hydration followed by an induction period before the main hydration peak at later times [52,53]. The dormant induction period is commonly observed for Portland cement, and thought to be related to a slow-down of the dissolution process due to low undersaturation [52,53]. The hydration process of the second peak reached its maximum value within 5–9 h. As expected, increasing the temperature from 20 °C to 40 °C accelerates the hydration reaction [54,55]. However, there is a reduction in heat flow at early ages (dissolution step). This is probably due to a faster approach to low undersaturation at higher temperatures. The second peak is much higher at 40 °C, due to the temperature-induced acceleration of the hydration reaction [54].

When exposed to an aqueous environment, the microcapsules retain water. St-DVB-PCM adsorbs water corresponding to 46% of its weight, while PE-EVA-PCM adsorbs 65% due to the more polar nature of the microcapsule shells [38]. This affects the effective water content in the samples, which has a complex effect on the reaction kinetics. Less available water in a system will normally cause a viscosity increase [56–58]. This has also been observed for pre-set Portland cement paste [41] and concrete [26], as well as for pre-set geopolymer paste [40] and concrete [26,38]. Since the components will move slower at higher viscosities (Stokes-Einstein relationship), it will take a longer time for the reactants to encounter each other. Accordingly, a viscosity increase may slow down the reaction rates [38]. On the other hand, a lower amount of available water will increase the effective concentration of the reactants, which may result in faster reaction rates [40]. In addition, for the geopolymers the rate of aluminosilicate dissolution is expected to increase when there is less water in the samples, due to the resulting higher concentration of OH^- [59]. A higher OH^- concentration might also speed up both the formation of geopolymer precursors and the polymerization of these precursors into the geopolymer network, since both these reactions involves OH^- as one of the reactants [40,60,61]. However, if the water retained by the microcapsules also includes the dissolved OH^- ions, the concentration of OH^- would not be affected and this effect could be neglectable. At very low water conditions the geopolymer reaction rate is expected to decrease when the available water is reduced, due to stabilization of the anions which reduce the rate of the condensation reactions [59]. A smaller water content will also lower the total amount of reactants that can be dissolved before the sample reaches saturation. Accordingly, low undersaturation will be approached faster, which may slow down the reaction. The different effects a reduced water content can have on the reaction rates is summarized in Table 5. The overall effect of MPCM addition (which decreases the available water) is expected to be a combination of these competing factors, and will depend on which factor that dominates in each case.

At 20 °C, MPCM addition to the geopolymer and Portland cement paste causes a decrease in the peak intensity of the first peak (Fig. 4). Significant amounts of water are retained by the MPCM particles [38], especially by PE-EVA-PCM (which contain polar groups). Since the peak reduction is more pronounced for PE-EVA-PCM, this suggests that the peak reduction is related to the adsorbed water. Less available water in the samples will lead to a faster approach to low undersaturation for the Portland cement and to less water for wetting and dissolution of FA and GGBFS in the geopolymer. This is expected to result in the observed reduced height of the first reaction peak.

While the first peak of the Portland cement stays more or less in the same place with the addition of MPCM, the first peak of the geopolymer samples are shifted towards longer times in the pres-

Table 5
The effect of decreased available water on the reaction rates. The arrows indicate increased (↑) or decreased (↓) reaction rates.

Decreasing available water	Geopolymer reaction rate	Portland cement reaction rate
Increased viscosity(until the samples has set)	↓	↓
Increased reactant concentrations(until saturation)	↑	↑
Increased rate of aluminosilicate dissolution(until saturation)	↑	–
Reduced rate of condensation reactions (very low water contents)	↓	–
Higher effective OH^- concentration	↑	–
Fewer reactants dissolved at saturation	↓	↓

ence of microcapsules. A lower availability of water is expected to increase the viscosity of the samples [40], which can slow down the formation of geopolymer precursors [38,62–64], thereby causing the observed shift of the first peaks toward longer times with MPCM addition.

Interestingly, at 40 °C both geopolymer and Portland cement containing 20% St-DVB-PCM have slightly higher heat evolution of the first peak than the samples without MPCM, while utilizing 20% PE-EVA-PCM still causes a reduction of the peaks. The reduction of the peak heights for PE-EVA-PCM is probably related to the high amount of adsorbed water (as discussed above). The reason for the higher first peak in the presence of ST-DVB-PCM at 40 °C is unclear. For geopolymers, the cumulative heat during this time period is lower for ST-DVB-PCM than for pure water (Fig. 5c). Accordingly, the total dissolution and reactions are reduced due to the lower water content in the presence of ST-DVB-PCM, while the peak becomes narrower and thereby higher (Fig. 4a). For Portland cement, the cumulative heat is initially higher for ST-DVB-PCM than in water (Fig. 5d), suggesting that early cement hydration is increased due to a higher concentration of reactants (Table 5).

For the geopolymer paste (Fig. 4a), the second peak is not markedly affected by MPCM addition. However, the overlap with the first peak makes it difficult to distinguish whether there are small changes. Since this reaction releases water instead of consuming it [65], it is less influenced by the available water in the sample (except for very low water contents [59]).

The second peak of Portland cement paste (Fig. 4b) is shifted toward longer times when MPCM is added to the samples. This prolongation of the dormant induction period is probably due to the water retained by the MPCM [38], which reduces the available water in the sample and thereby extend the period of low undersaturation.

As can be seen in Fig. 5a and c, there is a sharp increase in the cumulative heat immediately after starting the geopolymerization, which corresponds to the first peak of Fig. 4a. The total cumulative heat developed during the geopolymerization reaction is much higher at 40 °C than at 20 °C (Fig. 5a). The elevated temperature speeds up the alkaline activation of the geopolymer binder, causing the final products to form faster [66]. Since the reaction does not seem to be completed within the timeframe of the experiments, this causes a higher cumulative heat at 40 °C. At 20 °C, the MPCM is not significantly affecting the total amount of cumulative heat developed during the reaction. However, at 40 °C the sample containing St-DVB-PCM has the highest cumulative heat at long times while PE-EVA-PCM has the lowest. The reduced cumulative heat of PE-EVA-PCM is due to the lower amount of available water, causing higher viscosities and fewer reactants dissolved at saturation. This will slow down the reaction rates (Table 5), and thereby result in lower accumulated heat. The higher cumulative heat at long times for geopolymers containing St-DVB-PCM at 40 °C (Fig. 5a) is not evident at short times (Fig. 5c). This effect is therefore due to reactions occurring relatively late in the process, i.e., when the geopolymer precursors are combining into the 3D-geopolymer structure. Higher cumulative heat in the presence of St-DVB-PCM at 40 °C occurs only after the sample has set (Fig. 6a), and the viscosities are therefore not the dominating factor. It is possible that the reduced water content increases the effective concentration of OH^- in the sample [59], and that this speeds up the reaction between the geopolymer precursors and OH^- to form the geopolymer network.

For Portland cement paste (Fig. 5b and d), there is a small upturn of the cumulative heat at short times, corresponding to the first peak. This is followed by a period of slow increase (the dormant induction period) and a sharper upturn (the second peak) at longer times. As for the geopolymer paste, the total cumulative heat is higher at 40 °C than at 20 °C. The addition of microcapsules decreases the total accumulated heat at long times for both themperatures. This is probably caused by the

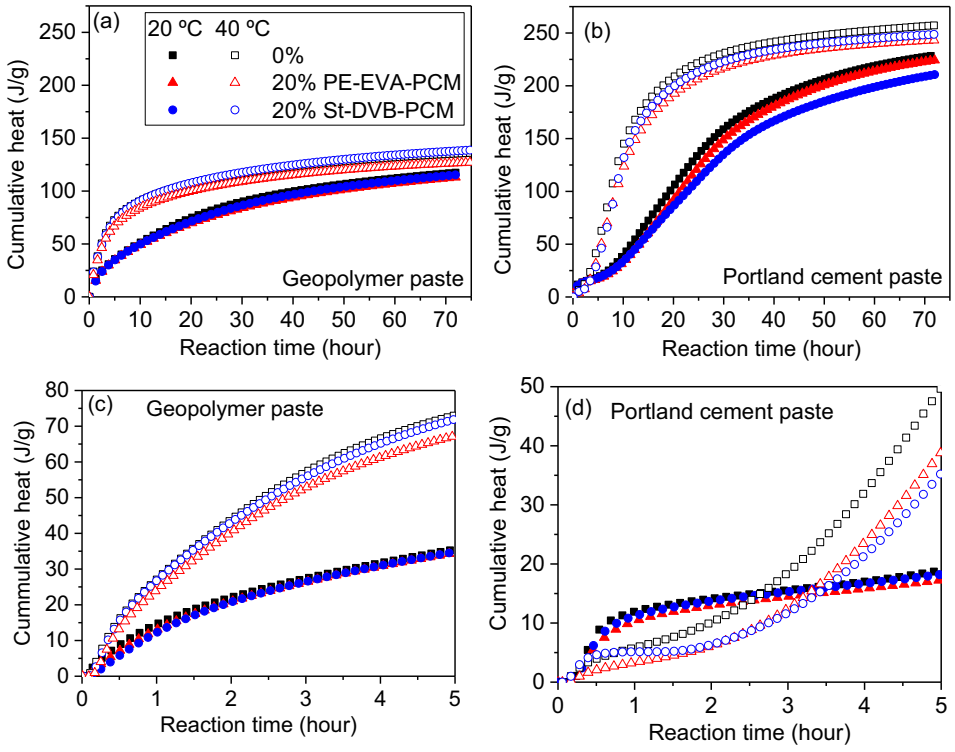

Fig. 5. Cumulative heat versus reaction time for (a) geopolymer paste during 72 h, (b) Portland cement paste during 72 h, (c) geopolymer paste during the first 5 h and (d) Portland cement paste during the first 5 h.

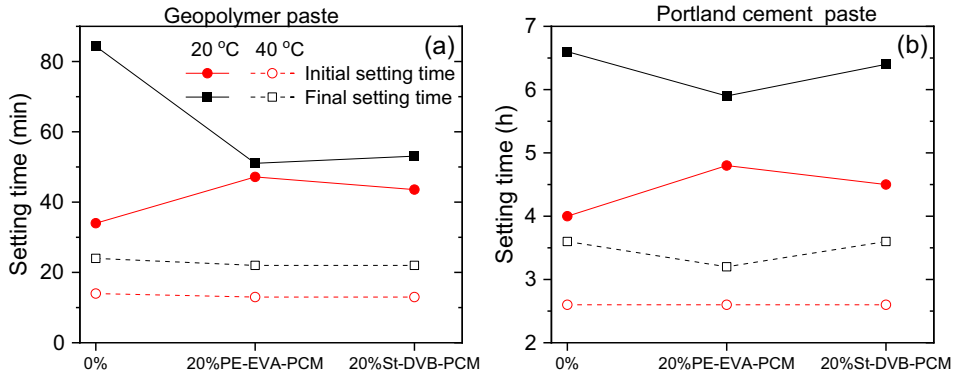

Fig. 6. The initial and final setting times of (a) geopolymer paste and (b) Portland cement paste containing 20 vol% of PE-EVA-PCM and St-DVB-PCM at 20 °C and 40 °C.

adsorption of water onto the MPCM, which can reduce the Portland cement hydration.

3.3. Setting time

The effect of MPCM and temperature on the initial and final setting times of geopolymer paste and Portland cement paste is illustrated in Fig. 6. As can be seen from Fig. 6a, the geopolymer reaction is significantly faster when the temperature is raised from 20 °C to 40 °C. As expected, the geopolymerization reaction is accelerated at higher temperatures without any significant effect of MPCM addition. When the temperature increases, the solubility of aluminosilicate is higher. This results in larger quantities of alumina and silica available for the geopolymerization reaction, speeding up the setting times of the geopolymer paste [67]. Unlike the setting times at 20 °C (which is discussed previously [38]), MPCM in liquid state (40 °C) has no noticeable effect on the setting times.

Fig. 6b shows that a higher temperature (40 °C) leads to rapid hydration and shorter setting times for Portland cement paste than at 20 °C [68]. At 20 °C, the initial setting time of Portland cement paste becomes longer in the presence of microcapsules due to the higher viscosity of the paste which leads to slower cement hydration [69]. However, at 40 °C MPCM addition has no significant effect on the initial setting time of cement. After the initial setting time, the solidification of the samples becomes faster in the presence of microcapsules, due to the water adsorption on the microcapsules surface [38]. For the final setting time at both 20 °C and 40 °C, the influence of PE-EVA-PCM is stronger than for St-DVB-PCM, since PE-EVA-PCM adsorbs higher amounts of water and has a smaller slump [38].

3.4. Compressive strength

The effects of temperature and MPCM addition on the compressive strength and compressive strength reduction of GPC and PCC are shown in Fig. 7. As observed previously [26], GPC has a higher compressive strength than PCC at both temperatures. In addition, the compressive strength of both GPC and PCC increase with curing time and temperature. For GPC, the higher temperature speeds up the formation of a hard structure, especially in the early-stage of the geopolymerization reaction [70]. Analogously, the faster hydration reaction increases the strength of PCC at elevated temperatures. At early curing times, the increase of the strength with temperature is more pronounced for the geopolymers, since the geopolymerization is faster than hydration at higher temperatures (Fig. 5).

The 28-day compressive strength (Fig. 7c, d) decreases with the addition of MPCM [26], and increases with temperature. In addition, it is smaller for PE-EVA-PCM than for St-DVB-PCM, except for 20% MPCM for PCC at 20 °C. PE-EVA-PCM has an irregular shell and form agglomerates, which may enhance the compressive strength reduction. In addition, we have previously demonstrated that more air is trapped within the PE-EVA-PCM samples, due to a reduced workability [38]. This lowers the compressive strength

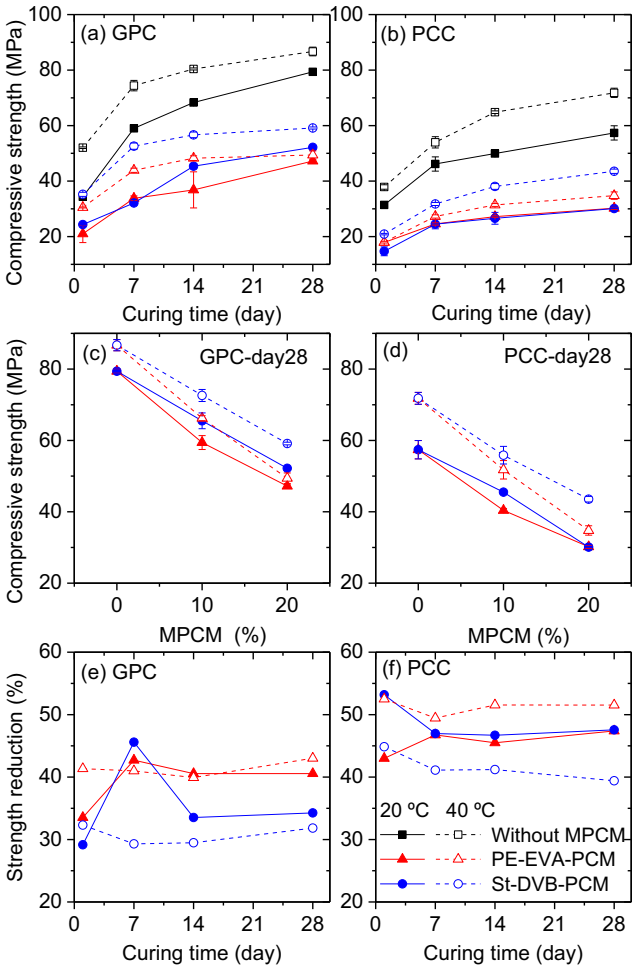

Fig. 7. Compressive strength at 20 and 40 °C as a function of curing time for (a) GPC with 20% MPCM and without MPCM, and (b) PCC with 20% MPCM and without MPCM, compressive strength of GPC and PCC as a function of the amount of sand replaced by MPCM after 28 days curing for (c) GPC, and (d) PCC. Reduction of compressive strength due to MPCM addition for (e) GPC with 20% MPCM and (f) PCC with 20% MPCM.

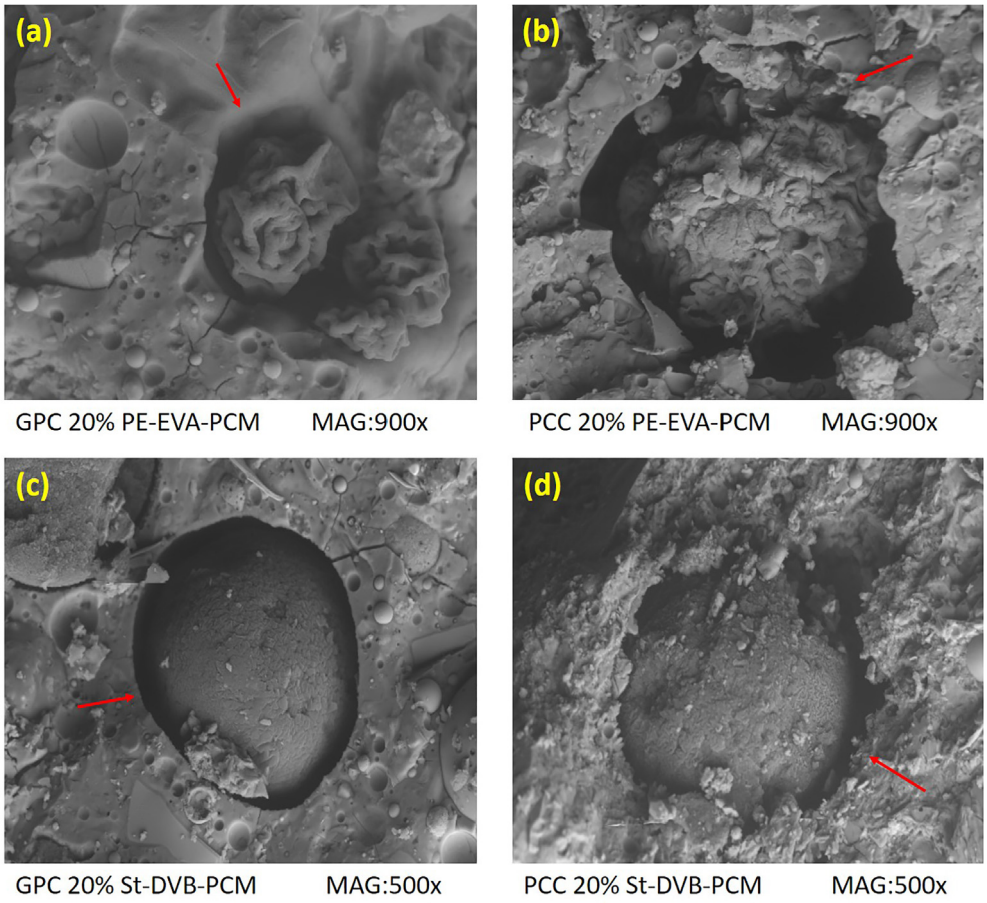

Fig. 8. SEM images of the fracture surface of (a) GPC containing 20% PE-EVA-PCM, (b) PCC containing 20% PE-EVA-PCM, (c) GPC containing 20% St-DVB-PCM, and (d) PCC containing 20% St-DVB-PCM. The arrows show the edge of shell-concrete matrix transition zone.

in comparison with St-DVB-PCM. Furthermore, PE-EVA-PCM contains significant amounts of non-encapsulated PCM [45], which might reduce the strength of the concrete.

The reduction of GPC and PCC compressive strength in the presence of 20% PE-EVA-PCM and St-DVB-PCM are shown in Fig. 7e and f. When cured at 20 °C, GPC has a stronger strength reduction at short curing times. However, after about 1 week it stabilizes at an approximately constant value. When cured at 40 °C, the reduction of GPC strength is almost constant at all curing ages. At long times, the strength reduction is approximately the same for the GPC samples cured at 20 and 40 °C, which is probably caused by the faster geopolymerization at higher temperatures (Fig. 5). The reduction of GPC strength is more pronounced for samples containing PE-EVA-PCM than for St-DVB-PCM. PCC containing PE-EVA-PCM and St-DVB-PCM show approximately the same strength reduction at 20 °C. However, for PCC cured at 40 °C the strength reduction is much higher in the presence of PE-EVA-PCM than for St-DVB-PCM. Melting the core of the microcapsules is expected to make them mechanically weaker, and therefore deteriorate the concrete strength. Interestingly, for PCC containing St-DVB-PCM the strength reduction is significantly lower at 40 °C than at 20 °C (Fig. 7f). This is probably caused by the higher mechanical strength of PCC cured at 40 °C (Fig. 7b), which makes it less vulnerable to softer particles. Comparing the temperature effects of the strength reductions of PCC and GPC, PCC is more affected by increasing the temperature above the melting point of the MPCM core than GPC. A more uniform and compact structure of GPC together with its initially higher mechanical strength may contribute to a better resistance against the softening of the particles.

3.5. Microstructural analysis

3.5.1. SEM imaging

SEM analysis was conducted on the failure surface of PCC and GPC samples containing 20% St-DVB-PCM and PE-EVA-PCM cured at 40 °C. Fig. 8 shows individual particles of St-DVB-PCM and PE-EVA-PCM in the GPC and PCC matrixes as an example of how the MPCMs shell binds with the surrounding matrix. Fig. 8 illustrates that there are more uniform and undamaged edges in the shell-concrete matrix transition zone of GPC than PCC. This illustrates a better compatibility between the MPCMs shell with GPC than for PCC. This might contribute to a better performance of GPC than PCC in the presence of MPCMs when the samples are exposed to temperature fluctuations from 20 °C to 40 °C or vice versa (Fig. 7a and b).

Smaller gaps are observed at the interface between St-DVB-PCM and the concrete matrix compared to PE-EVA-PCM, suggesting a better compatibility between the St-DVB-PCM shells and the surrounding matrix. The larger gaps combined with agglomeration of PE-EVA-PCM [45,71] and non-encapsulated PCMs in the PE-EVA-PCM samples [45] contributes to the greater reduction of PE-EVA-PCM compressive strength compared to St-DVB-PCM [38].

3.5.2. X-ray micro-tomography

Typical 2D X-ray micro-tomography cross-sectional slices of GPC and PCC without MPCMs cured at 20 °C and 40 °C are depicted in Fig. 9. To obtain reliable statistical data, more than 600 2D slices were taken for each sample. As seen in Fig. 9a and b, more air voids are visible in the GPC samples cured at 40 °C than at 20 °C. Increas-

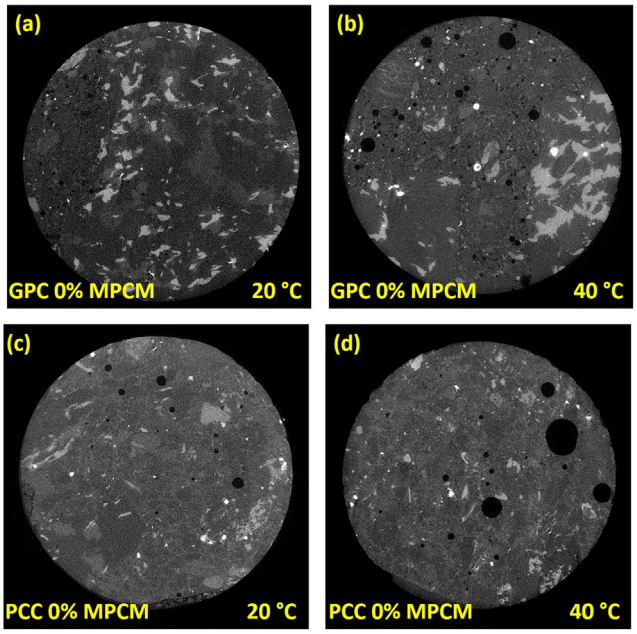

Fig. 9. X-ray-tomography images of (a) GPC without MPCM at 20 °C, (b) GPC without MPCM at 40 °C, (c) PCC without MPCM at 20 °C, and (d) PCC without MPCM at 40 °C. Dark colors indicate low or no absorption of X-rays (e.g. microcapsules or air bubbles) and bright colors indicate high absorption of X-rays (gravel and sand). The images have approximately 1 cm field of view.

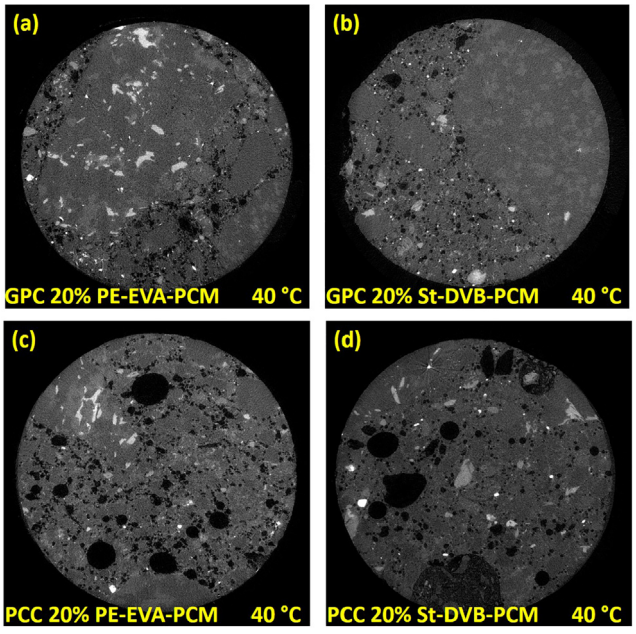

Fig. 10. X-ray-tomography images of (a) GPC containing 20% PE-EVA-PCM, (b) GPC containing 20% St-DVB-PCM, (c) PCC containing 20% PE-EVA-PCM, and (d) PCC containing 20% St-DVB-PCM at 40 °C. Dark colors indicate low or no absorption of X-rays (e.g. microcapsules or air bubbles) and bright colors indicate high absorption of X-rays (gravel and sand). The images have approximately 1 cm field of view.

ing the curing temperature is known to dissolve more Si and Al from the amorphous phases. This accelerates the development of a hard structure, especially during the initial stages of the geopolymerization reaction. Accordingly, higher temperature increases water evaporation rates thereby producing further air voids [72]. This causes the formation of micro-cavities, and therefore an increase in the porosity of the GPC matrix. For PCC, higher temperatures enhance the hydration rates. This results in a more heterogeneous hydration distribution, and enhanced porosity. Lower temperatures results in a more homogenous and uniform distribution of the hydrates, and thereby the formation of smaller pores [73].

Fig. 10 shows the distribution of the MPCMs in the GPC and PCC matrix. Given the low level of X-ray attenuation of the MPCMs, it is challenging to utilize grey scale values to distinguish between air voids and microcapsules. However, since air voids tend to be spherical, irregular profiles are probably due to agglomerated MPCM. Fig. 10 shows that both agglomerated St-DVB-PCM and PE-EVA-PCM are distributed throughout the PCC samples. GPC has some regions containing agglomerated MPCMs and some more homogeneous regions without any MPCMs distribution. The enhanced viscosity (reduced workability) of the fresh GPC and the fast setting times of GPC especially at 40 °C can contribute to the prevention of a homogeneous distribution of MPCM throughout the matrix.

4. Conclusion

Incorporation of PCMs in building materials can help reduce the energy needed to heat and cool buildings, while retaining a comfortable indoor temperature. However, inclusion of PCMs in construction materials influence many aspects of their performance. In this paper, the influence of two different MPCMs in liquid and solid state (above and below the melting point of the PCM core) on the reaction kinetics, physical, mechanical and microstructural properties of Portland cement and geopolymer concrete/pastes were investigated. The following conclusions can be drawn from this work:

1. The microcapsules shell can resist the highly basic nature of the alkaline solution without any leakage or damage. A few microcapsules were broken and damaged during the mixing process due to the lower stiffness and strength of the MPCM shell compared to the conventional aggregates.
2. Isothermal calorimetry shows that MPCM addition slows down the reaction of both geopolymer and Portland cement paste at 20 °C, which is probably due to the water adsorption onto the microcapsules. At 40 °C, the effect of microcapsule addition is more complex, and St-DVB-PCM are speeding up some of the reactions.
3. The setting times of geopolymer paste and Portland cement paste were accelerated at higher temperatures due to faster geopolymerization and hydration. MPCM in liquid state (40 °C) has no noticeable effect on the setting times of geopolymer paste. For Portland cement paste, PE-EVA-PCM has a greater influence on the final setting time than St-DVB-PCM, since much more water are adsorbed onto PE-EVA-PCM.
4. The compressive strength of both GPC and PCC increased with curing time and temperature. However, MPCMs addition reduced the compressive strength, and heating the samples above the melting point of the MPCM core affected PCC much more than GPC. The strength reduction was more pronounced for PE-EVA-PCM than for St-DVB-PCM. The irregular shell, agglomeration, and reduced workability of PE-EVA-PCM are probably the major contributing factors for this.
5. A more uniform and compact structure of GPC combined with higher mechanical strength might contribute to the better resistance against softer particles. There were more uniform and undamaged edges in the shell-concrete matrix transition zone of GPC than for PCC. This might contribute to the better perfor-

mance of GPC than PCC when microcapsules are added to the samples. Porosity was enhanced at higher temperatures in both GPC and PCC. Increased viscosity (poorer workability) of the fresh GPC and the fast setting times of GPC especially at 40 °C may contribute to the prevention of a homogeneous distribution of MPCM throughout the matrix.

CRediT authorship contribution statement

Shima Pilehvar: Conceptualization, Methodology, Validation, Investigation, Writing - original draft, Writing - review & editing. **Susana G. Sanfelix:** Investigation, Writing - review & editing. **Anna M. Szczotok:** Investigation, Writing - review & editing. **Juan Francisco Rodríguez:** Investigation, Writing - review & editing. **Luca Valentini:** Investigation, Writing - review & editing, Visualization. **Marcos Lanzón:** Investigation, Writing - review & editing, Visualization. **Ramón Pamies:** Writing - review & editing, Visualization, Supervision. **Anna-Lena Kjøniksen:** Resources, Writing - review & editing, Visualization, Supervision, Project administration, Funding acquisition.

Declaration of Competing Interest

The authors declare that they have no known competing financial interests or personal relationships that could have appeared to influence the work reported in this paper.

Acknowledgement

We gratefully acknowledge funding from the Research Council of Norway, project number 238198. The authors acknowledge Fundación Séneca Agencia de Ciencia y Tecnología de la Región de Murcia "Ayuda a las Unidades y Grupos de Excelencia Científica de la Región de Murcia (Programa Séneca 2014)" (Grant # 19877/GERM/14), for financial support.

References

[1] E. Benhelal, G. Zahedi, E. Shamsaei, A. Bahadori, Global strategies and potentials to curb CO2 emissions in cement industry, J. Cleaner Prod. 51 (2013) 142–161.
[2] J. Davidovits, Geopolymers: inorganic polymeric new materials, J. Therm. Anal. Calorim. 37 (8) (1991) 1633–1656.
[3] J. Davidovits, Geopolymer Chemistry and Applications, Institute Géopolymère, Saint-Quentin, France, 2011.
[4] C.K. Yip, G.C. Lukey, J.L. Provis, J.S.J. van Deventer, Effect of calcium silicate sources on geopolymerisation, Cem. Concr. Res. 38 (4) (2008) 554–564.
[5] E.I. Diaz, E.N. Allouche, S. Eklund, Factors affecting the suitability of fly ash as source material for geopolymers, Fuel 89 (5) (2010) 992–996.
[6] P. Nath, P.K. Sarker, Effect of GGBFS on setting, workability and early strength properties of fly ash geopolymer concrete cured in ambient condition, Constr. Build. Mater. 66 (2014) 163–171.
[7] S. Thokchom, D. Dutta, S. Ghosh, Effect of incorporating silica fume in fly ash geopolymers, World Academy of Science, Engineering and Technology 60 (2011) 243–247.
[8] G.S. Ryu, Y.B. Lee, K.T. Koh, Y.S. Chung, The mechanical properties of fly ash-based geopolymer concrete with alkaline activators, Constr. Build. Mater. 47 (2013) 409–418.
[9] Y. Fu, L. Cai, W. Yonggen, Freeze–thaw cycle test and damage mechanics models of alkali-activated slag concrete, Constr. Build. Mater. 25 (7) (2011) 3144–3148.
[10] D. Urge-Vorsat, K. Petrichenko, M. Antal, M. Staniec, E. Ozden, E. Labzina, M. Labelle, Best Practice Policies for Low Carbon & Energy Buildings. A Scenario Analysis., Global Buildings Performance Network ,Budapest (2012).
[11] J. Giro-Paloma, M. Martínez, L.F. Cabeza, A.I. Fernández, Types, methods, techniques, and applications for microencapsulated phase change materials (MPCM): A review, Renew. Sustain. Energy Rev. 53 (2016) 1059–1075.
[12] A.M. Khudhair, M.M. Farid, A review on energy conservation in building applications with thermal storage by latent heat using phase change materials, Energy Convers. Manage. 45 (2) (2004) 263–275.
[13] V.V. Tyagi, D. Buddhi, PCM thermal storage in buildings: A state of art, Renew. Sustain. Energy Rev. 11 (6) (2007) 1146–1166.
[14] T.-C. Ling, C.-S. Poon, Use of phase change materials for thermal energy storage in concrete: An overview, Constr. Build. Mater. 46 (2013) 55–62.
[15] H. Akeiber, P. Nejat, M.Z.A. Majid, M.A. Wahid, F. Jomehzadeh, I. Zeynali Famileh, J.K. Calautit, B.R. Hughes, S.A. Zaki, A review on phase change material (PCM) for sustainable passive cooling in building envelopes, Renew. Sustain. Energy Rev. 60 (2016) 1470–1497.
[16] S.E. Kalnæs, B.P. Jelle, Phase change materials and products for building applications: A state-of-the-art review and future research opportunities, Energy Build. 94 (2015) 150–176.
[17] N. Zhu, Z. Ma, S. Wang, Dynamic characteristics and energy performance of buildings using phase change materials: A review, Energy Convers. Manage. 50 (12) (2009) 3169–3181.
[18] A. de Gracia, L.F. Cabeza, Phase change materials and thermal energy storage for buildings, Energy and Buildings 103(Supplement, C) (2015) 414–419.
[19] D. Zhou, C.Y. Zhao, Y. Tian, Review on thermal energy storage with phase change materials (PCMs) in building applications, Applied Energy 92 (Supplement C) (2012) 593–605.
[20] M.N.A. Hawlader, M.S. Uddin, M.M. Khin, Microencapsulated PCM thermal-energy storage system, Appl. Energy 74 (1–2) (2003) 195–202.
[21] A. Eddhahak-Ouni, S. Drissi, J. Colin, J. Neji, S. Care, Experimental and multi-scale analysis of the thermal properties of Portland cement concretes embedded with microencapsulated Phase Change Materials (PCMs), Appl. Therm. Eng. 64 (1–2) (2014) 32–39.
[22] L.F. Cabeza, C. Castellón, M. Nogués, M. Medrano, R. Leppers, O. Zubillaga, Use of microencapsulated PCM in concrete walls for energy savings, Energy Build. 39 (2) (2007) 113–119.
[23] A. Figueiredo, J. Lapa, R. Vicente, C. Cardoso, Mechanical and thermal characterization of concrete with incorporation of microencapsulated PCM for applications in thermally activated slabs, Constr. Build. Mater. 112 (2016) 639–647.
[24] T. Lecompte, P. Le Bideau, P. Glouannec, D. Nortershauser, S. Le Masson, Mechanical and thermo-physical behaviour of concretes and mortars containing phase change material, Energy Build. 94 (2015) 52–60.
[25] M. Hunger, A. Entrop, I. Mandilaras, H. Brouwers, M. Founti, The behavior of self-compacting concrete containing micro-encapsulated phase change materials, Cem. Concr. Compos. 31 (10) (2009) 731–743.
[26] S. Pilehvar, V.D. Cao, A.M. Szczotok, L. Valentini, D. Salvioni, M. Magistri, R. Pamies, A.-L. Kjøniksen, Mechanical properties and microscale changes of geopolymer concrete and Portland cement concrete containing micro-encapsulated phase change materials, Cem. Concr. Res. 100 (2017) 341–349.
[27] S.H. Kosmatka, B. Kerkhoff, W.C. Panarese, N.F. MacLeod, R.J. McGrath, Design and Control of Concrete Mixtures, Seventh Canadian Edition, Cement Association of Canada (2002) 151.
[28] R. Shadnia, L. Zhang, P. Li, Experimental study of geopolymer mortar with incorporated PCM, Constr. Build. Mater. 84 (2015) 95–102.
[29] Z. Wang, H. Su, S. Zhao, N. Zhao, Influence of phase change material on mechanical and thermal properties of clay geopolymer mortar, Constr. Build. Mater. 120 (2016) 329–334.
[30] H. Zhang, F. Xing, H.-Z. Cui, D.-Z. Chen, X. Ouyang, S.-Z. Xu, J.-X. Wang, Y.-T. Huang, J.-D. Zuo, J.-N. Tang, A novel phase-change cement composite for thermal energy storage: Fabrication, thermal and mechanical properties, Appl. Energy 170 (2016) 130–139.
[31] V.D. Cao, T.Q. Bui, A.-L. Kjøniksen, Thermal analysis of multi-layer walls containing geopolymer concrete and phase change materials for building applications, Energy 186 (2019) 115792.
[32] V.D. Cao, S. Pilehvar, C. Salas-Bringas, A.M. Szczotok, T.Q. Bui, M. Carmona, J.F. Rodriguez, A.-L. Kjøniksen, Thermal performance and numerical simulation of geopolymer concrete containing different types of thermoregulating materials for passive building applications, Energy Build. 173 (2018) 678–688.
[33] V.D. Cao, S. Pilehvar, C. Salas-Bringas, A.M. Szczotok, T.Q. Bui, M. Carmona, J.F. Rodriguez, A.-L. Kjøniksen, Thermal analysis of geopolymer concrete walls containing microencapsulated phase change materials for building applications, Sol. Energy 178 (2019) 295–307.
[34] V.D. Cao, S. Pilehvar, C. Salas-Bringas, A.M. Szczotok, J.F. Rodriguez, M. Carmona, N. Al-Manasir, A.-L. Kjøniksen, Microencapsulated phase change materials for enhancing the thermal performance of Portland cement concrete and geopolymer concrete for passive building applications, Energy Convers. Manage. 133 (2017) 56–66.
[35] V.D. Cao, S. Pilehvar, C. Salas-Bringas, A.M. Szczotok, L. Valentini, M. Carmona, J.F. Rodriguez, A.-L. Kjøniksen, Influence of microcapsule size and shell polarity on thermal and mechanical properties of thermoregulating geopolymer concrete for passive building applications, Energy Convers. Manage. 164 (2018) 198–209.
[36] X. Pang, W.C. Jimenez, V. Goel, Use of Microencapsulated Phase-Change Materials To Regulate the Temperature of Oilwell Cement, SPE-20926-PA 31 (1) (2016).
[37] B.A. Young, G. Falzone, Z. She, A.M. Thiele, Z. Wei, N. Neithalath, G. Sant, L. Pilon, Early-age temperature evolutions in concrete pavements containing microencapsulated phase change materials, Constr. Build. Mater. 147 (2017) 466–477.
[38] S. Pilehvar, V.D. Cao, A.M. Szczotok, M. Carmona, L. Valentini, M. Lanzón, R. Pamies, A.-L. Kjøniksen, Physical and mechanical properties of fly ash and slag geopolymer concrete containing different types of micro-encapsulated phase change materials, Constr. Build. Mater. 173 (2018) 28–39.
[39] S. Pilehvar, A.M. Szczotok, J.F. Rodríguez, L. Valentini, M. Lanzón, R. Pamies, A.-L. Kjøniksen, Effect of freeze-thaw cycles on the mechanical behavior of geopolymer concrete and Portland cement concrete containing micro-encapsulated phase change materials, Constr. Build. Mater. 200 (2019) 94–103.

[40] V.D. Cao, S. Pilehvar, C. Salas-Bringas, A.M. Szczotok, N.B.D. Do, H.T. Le, M. Carmona, J.F. Rodriguez, A.-L. Kjøniksen, Influence of Microcapsule Size and Shell Polarity on the Time-Dependent Viscosity of Geopolymer Paste, Ind. Eng. Chem. Res. 57 (29) (2018) 9457–9464.
[41] S.G. Sanfelix, I. Santacruz, A.M. Szczotok, L.M.O. Belloc, A.G. De la Torre, A.-L. Kjøniksen, Effect of microencapsulated phase change materials on the flow behavior of cement composites, Constr. Build. Mater. 202 (2019) 353–362.
[42] A.M. Borreguero, J.L. Valverde, J.F. Rodríguez, A.H. Barber, J.J. Cubillo, M. Carmona, Synthesis and characterization of microcapsules containing Rubitherm®RT27 obtained by spray drying, Chem. Eng. J. 166 (1) (2011) 384–390.
[43] A.M. Szczotok, M. Carmona, A.-L. Kjøniksen, J.F. Rodriguez, Equilibrium adsorption of polyvinylpyrrolidone and its role on thermoregulating microcapsules synthesis process, Colloid Polym. Sci. 295 (5) (2017) 783–792.
[44] M. Saffari, A. de Gracia, C. Fernández, L.F. Cabeza, Simulation-based optimization of PCM melting temperature to improve the energy performance in buildings, Appl. Energy 202 (2017) 420–434.
[45] V.D. Cao, C. Salas-Bringas, R.B. Schüller, A.M. Szczotok, M. Hiorth, M. Carmona, J.F. Rodriguez, A.-L. Kjøniksen, Rheological and thermal properties of suspensions of microcapsules containing phase change materials, Colloid Polym. Sci. 296 (5) (2018) 981–988.
[46] P. Meshgin, Y. Xi, Effect of Phase-Change Materials on Properties of Concrete, Aci Mater J 109 (6) (2012) 685–686.
[47] J. Giro-Paloma, C. Barreneche, A. Maldonado-Alameda, M. Royo, J. Formosa, A.I. Fernández, J.M. Chimenos, Alkali-Activated Cements for TES Materials in Buildings' Envelops Formulated With Glass Cullet Recycling Waste and Microencapsulated Phase Change Materials, Materials 12 (13) (2019) 2144.
[48] S.K. Nath, S. Mukherjee, S. Maitra, S. Kumar, Kinetics study of geopolymerization of fly ash using isothermal conduction calorimetry, J. Therm. Anal. Calorim. 127 (3) (2017) 1953–1961.
[49] B. Singh, M.R. Rahman, R. Paswan, S.K. Bhattacharyya, Effect of activator concentration on the strength, ITZ and drying shrinkage of fly ash/slag geopolymer concrete, Constr. Build. Mater. 118 (2016) 171–179.
[50] C. Tennakoon, R.S. Nicolas, J.G. Sanjayan, A. Shayan, Thermal effects of activators on the setting time and rate of workability loss of geopolymers, Ceram. Int. 42 (16) (2016) 19257–19268.
[51] E.N. Kani, A. Allahverdi, J.L. Provis, Calorimetric study of geopolymer binders based on natural pozzolan, J. Therm. Anal. Calorim. 127 (3) (2017) 2181–2190.
[52] P. Juilland, E. Gallucci, R. Flatt, K. Scrivener, Dissolution theory applied to the induction period in alite hydration, Cem. Concr. Res. 40 (6) (2010) 831–844.
[53] K.L. Scrivener, P. Juilland, P.J.M. Monteiro, Advances in understanding hydration of Portland cement, Cem. Concr. Res. 78 (2015) 38–56.
[54] E. Gruyaert, N. Robeyst, N. De Belie, Study of the hydration of Portland cement blended with blast-furnace slag by calorimetry and thermogravimetry, J. Therm. Anal. Calorim. 102 (3) (2010) 941–951.
[55] H. Kada-Benameur, E. Wirquin, B. Duthoit, Determination of apparent activation energy of concrete by isothermal calorimetry, Cem. Concr. Res. 30 (2) (2000) 301–305.
[56] J.W. Bullard, A.T. Pauli, E.J. Garboczi, N.S. Martys, A comparison of viscosity–concentration relationships for emulsions, J. Colloid Interface Sci. 330 (1) (2009) 186–193.
[57] T.F. Ford, Viscosity-concentration and fluidity-concentration relationships for suspensions of spherical particles in newtonian liquids, J. Phys. Chem. 64 (9) (1960) 1168–1174.
[58] F.L. Saunders, Rheological properties of monodisperse latex systems I. Concentration dependence of relative viscosity, J. Colloid Sci. 16 (1) (1961) 13–22.
[59] J.L. Provis, J.S.J. van Deventer, Geopolymerisation kinetics. 2. Reaction kinetic modelling, Chem. Eng. Sci. 62 (9) (2007) 2318–2329.
[60] K.-T. Wang, Q. Tang, X.-M. Cui, Y. He, L.-P. Liu, Development of near-zero water consumption cement materials via the geopolymerization of tektites and its implication for lunar construction, Sci. Rep. 6 (2016) 29659.
[61] A.M. Mustafa Al Bakri, H. Kamarudin, M. Bnhussain, I. Khairul Nizar, W.I.W. Mastura, Mechanism and Chemical Reaction of Fly Ash Geopolymer Cement- A Review, Journal of Asian Scientific Research 1 (2011) 247-253.
[62] A. Kumar, S.S. Pawar, High viscosity of ionic liquids causes rate retardation of Diels-Alder reactions, Science China Chemistry 55 (8) (2012) 1633–1637.
[63] U. Rattanasak, P. Chindaprasirt, Influence of NaOH solution on the synthesis of fly ash geopolymer, Miner. Eng. 22 (12) (2009) 1073–1078.
[64] I. Pane, W. Hansen, Investigation of blended cement hydration by isothermal calorimetry and thermal analysis, Cem. Concr. Res. 35 (6) (2005) 1155–1164.
[65] H. Xu, J.S.J. Van Deventer, The geopolymerisation of alumino-silicate minerals, Int. J. Miner. Process. 59 (3) (2000) 247–266.
[66] S. Alonso, A. Palomo, Alkaline activation of metakaolin and calcium hydroxide mixtures: influence of temperature, activator concentration and solids ratio, Mater. Lett. 47 (1–2) (2001) 55–62.
[67] A.A. Siyal, K.A. Azizli, Z. Man, H. Ullah, Effects of Parameters on the Setting Time of Fly Ash Based Geopolymers Using Taguchi Method, Procedia Eng. 148 (2016) 302–307.
[68] J.I. Escalante-García, J.H. Sharp, Effect of temperature on the hydration of the main clinker phases in portland cements: part i, neat cements, Cem. Concr. Res. 28 (9) (1998) 1245–1257.
[69] D.P. Bentz, Influence of water-to-cement ratio on hydration kinetics: Simple models based on spatial considerations, Cem. Concr. Res. 36 (2) (2006) 238–244.
[70] P. Rovnaník, Effect of curing temperature on the development of hard structure of metakaolin-based geopolymer, Constr. Build. Mater. 24 (7) (2010) 1176–1183.
[71] V.D. Cao, C. Salas-Bringas, R. Barfod Schüller, A.M. Szczotok, A.-L. Kjøniksen, Time-dependent structural breakdown of microencapsulated phase change materials suspensions, J. Dispersion Sci. Technol. 40 (2) (2019) 179–185.
[72] M.S. Muñiz-Villarreal, A. Manzano-Ramírez, S. Sampieri-Bulbarela, J.R. Gasca-Tirado, J.L. Reyes-Araiza, J.C. Rubio-Ávalos, J.J. Pérez-Bueno, L.M. Apatiga, A. Zaldivar-Cadena, V. Amigó-Borrás, The effect of temperature on the geopolymerization process of a metakaolin-based geopolymer, Mater. Lett. 65 (6) (2011) 995–998.
[73] B. Lothenbach, F. Winnefeld, C. Alder, E. Wieland, P. Lunk, Effect of temperature on the pore solution, microstructure and hydration products of Portland cement pastes, Cem. Concr. Res. 37 (4) (2007) 483–491.